WP5.1: Conduct and Analytical Support to Air Ingress Experiment QUENCH-16

J. BIRCHLEY[1], L. FERNANDEZ MOGUEL[1], C. BALS[2], E. BEUZET[3], Z. HOZER[4], J. STUCKERT[5]

[1] PSI, Villigen (CH) [2] GRS, Garching (DE) [3] EDF, Clamart (FR)
[4] AEKI, Budapest (HU) [5] KIT, Karlsruhe (DE)

ABSTRACT

Air ingress experiment QUENCH-16 was performed by KIT to extend the currently existing database on the transient behaviour during air ingress on a dried out and partially oxidised bundle. An earlier experiment, QUENCH-10 studied the effect of air ingress on an extensively pre-oxidised bundle, while QUENCH-16 examined the behaviour following mild preoxidation. A primary test objective was to investigate nitride formation during prolonged oxygen starvation to provide conditions for studying the reaction between partially oxidised cladding and nitrogen. The experiment was performed within the EU part-sponsored LACOMECO programme, and was proposed and partnered by the Hungarian Institute, AEKI.

Extensive pre-test analytical support was provided by GRS (ATHLET-CD), EDF (MAAP4) and PSI (SCDAPSim and MELCOR-186) to determine test conditions to meet the objectives, taking into account the uncertainties concerning air oxidation behaviour. The different treatments of air oxidation modelling provided mutual confirmation of the predicted behaviour. The inlet flow was specified at 3 g/s steam and 3 g/s argon during pre-oxidation and 0.2 g/s air and 1 g/s argon during the air ingress. The low flow rates during the air phase were chosen to result in oxygen starvation early enough to achieve the long starvation period.

The experiment was successfully conducted at KIT on 27 July 2011. Mild preoxidation was followed by a planned cooldown before the switch to air flow which initiated a gradual temperature rise which accelerated as more and more of the oxygen was consumed. During the period of complete consumption some of the nitrogen was consumed and zirconium nitride was formed. A strong oxidation excursion took place during the reflood, possibly triggered by the degraded state of the oxide layer due to the oxygen starvation and the reaction with nitrogen. Preliminary post-test analyses are underway by the above participants and also by IRSN using ICARE-CATHARE, and will be the subject of a future paper.

1 INTRODUCTION

Air ingress issues, first raised by Powers et al. [1], have received considerable attention in recent years in view of the likely acceleration in the cladding oxidation, fuel rod degradation, and the release of some fission products, most notable ruthenium. This last issue is being addressed within the SARNET2 Source Term Work Package. In addition, the Paks NPP cleaning tank incident and the accident at Fukushima Daiichi drew attention to the possibility of overheated fuel assemblies becoming exposed to air outside of the reactor.

As a consequence, air ingress is the subject of recent and continuing multinational efforts, notably within the European Union 6th Framework SARNET project [2], the MOZART experiments [3] within the ongoing International Source Term Programme (ISTP) [4], numerous investigations at KIT [5], [6], AEKI [7]. Elsewhere ANL performed a large

programme of experiments [8] and the OECD Sandia Fuel Project [9] was recently launched. A number of previous integral air ingress experiments have been performed under a range of configurations and oxidising conditions, namely AIT-1, AIT-2 [10], QUENCH-10 [11], [12] and PARAMETER SF4 [13]. The accumulated data has demonstrated that air oxidation is a remarkably complicated phenomena governed by numerous processes whose role can depend critically on the oxidising conditions, the past oxidation history and the details of the cladding material specification. The knowledge and models for air oxidation do not yet cover the whole range of representative conditions. The post-test analyses of integral experiments and the safety analyses of severe accidents with air ingress scenarios showed that fast oxidation and temperature excursion can be initiated by relatively small effects in high temperature air. From both scientific and accident management points of view it should be identified under which conditions the temperature excursion could be prevented and the damage of bundle could be limited in air ingress scenarios. The main aims of QUENCH-16 were to investigate areas where data were comparatively sparse.

The QUENCH-16 test was proposed [14] in the frame of the EC-sponsored LACOMECO programme [15], [16] as part of the collective investigation of air ingress into overheated nuclear fuel assemblies. The experiment would focus specifically of following phenomena:

- air oxidation after rather moderate pre-oxidation in steam;
- slow oxidation and nitriding of zirconium in high temperature air and transition to rapid oxidation and temperature excursion;
- role of nitrogen under oxygen-starved conditions,
- formation of oxide and nitride layers on the surface of Zr;
- release of hydrogen from oxidised zirconium during air ingress scenario;
- reflooding of oxidised and nitrided bundle by water, release of nitrogen.

The above scientific objectives were defined in the proposed scenario and agreed by the LACOMECO experiment selection panel [17]. The proposal included a target scenario characterised by:

- a long period of oxygen starvation to promote the occurrence of the above phenomena;
- reflood quench initiated at temperatures well below the melting point of the cladding to provide the opportunity of avoiding a major oxidation, to facilitate post-test inspection of the bundle.

Concerning the second, it was realised that avoiding such an excursion could not be guaranteed, especially in the light of previous experiments such as PARAMETER-SF4 which showed clearly how a starvation period can promote an excursion. The outcome would in any case yield valuable data on this phenomenon.

QUENCH-16 was successfully performed by KIT on 27 July 2011, according to a test protocol agreed following discussions among the participants and based on coordinated planning analyses by GRS, EDF and PSI using independent simulation tools. This paper describes the objectives, planning analyses and conduct of QUENCH-16, identifies the questions raised by the test results, and the future plans for post test analysis and interpretation.

2 SUMMARY OF QUENCH-16 (KIT)

2.1 QUENCH facility

The main component of the QUENCH test facility is the test section with the test bundle (Figure 1). The facility can be operated in two modes: a forced-convection mode (typical for most QUENCH experiments) and a boil-off mode. QUENCH-16 was conducted in forced-convection mode, in which, superheated steam from the steam generator and superheater together with argon as a carrier gas for off-gas measurements enter the test bundle at the

bottom. The system pressure in the test section is around 0.2 MPa absolute. The test section has separate inlets at the bottom to inject water for reflood (bottom quenching) and synthetic air (80% N_2 and 20% O_2) during air ingress phase. The argon, the steam not consumed, and the hydrogen produced in the zirconium-steam reaction flow from the bundle outlet at the top through a water-cooled off-gas pipe to the condenser where the steam is separated from the non-condensable gases. The water cooling circuits for bundle head and off-gas pipe are temperature-controlled to guarantee that the steam/gas temperature is high enough so that condensation at the test section outlet and inside the off-gas pipe is avoided.

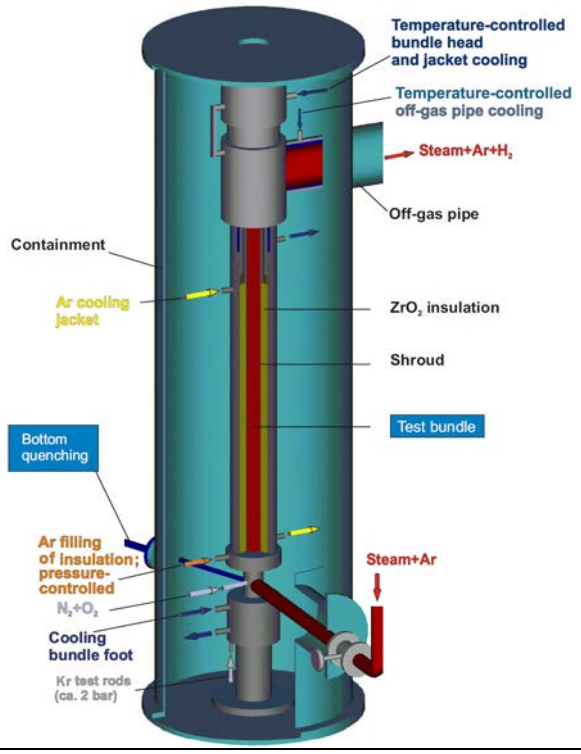

Figure 1. Containment and test section.

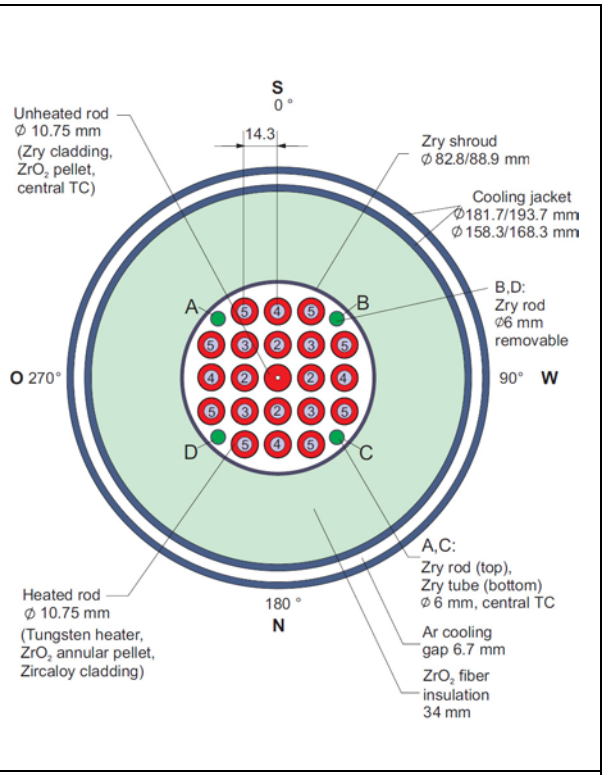

Figure 2. Bundle cross section.

The test bundle is approximately 2.5 m long and is made up of 21 fuel rod simulators (Figure 2). The fuel rod simulators are held in position by five grid spacers, four are made of Zircaloy-4 and the one at the bottom of Inconel 718. Except the central one all rods are heated. Heating is electric by 6 mm diameter tungsten heaters of length 1024 mm installed in the rod centre (lower edge of heaters corresponds to bundle elevation 0 mm). Electrodes of molybdenum (length 300 + 576 mm; Ø 8.6 mm) and copper (length 390 + 190 mm; Ø 8.6 mm) are connected to the tungsten heaters at one end and to the cable leading to the DC electrical power supply at the other end. The measured electrical power includes the heat dissipation at cables. The heating power inside the bundle is distributed between two groups of heated rods. The distribution of the electric power within the two groups is as follows: about 40 % of the power is released into the inner rod circuit consisting of eight fuel rod simulators (in parallel connection) and 60 % in the outer rod circuit (12 fuel rod simulators in parallel connection). The tungsten heaters are surrounded by annular ZrO_2-TZP pellets. The rod cladding of the heated and unheated fuel rod simulators is Zircaloy-4 with 10.75 mm outside diameter and 0.725 mm wall thickness. All test rods are filled with Kr at a pressure of approx. 0.22 MPa absolute. The rods were connected to a controlled feeding system that compensated minor gas losses and allowed observation of the first cladding failure as well as a failure progression.

There are four corner rods installed in the bundle. Two of them, i.e. rods "A" and "C", are made of a Zircaloy-4 solid rod at the top and a Zircaloy-4 tube at the bottom and are used for thermocouple instrumentation. The other two rods, i.e. rods "B" and "D" (solid Zircaloy-4 rods of 6 mm diameter) are particularly designed to be withdrawn from the bundle to check the amount of ZrO_2 oxidation and hydrogen uptake at specific times. Rod B was pulled out of the bundle before the air ingress phase of the experiment and rod D was pulled before quenching; low part of rod A was removed after test termination.

The test bundle is surrounded by a 3.05 mm shroud of Zirconium-702 (inner diameter 82.8 mm) with a 34 mm thick ZrO_2 fibre insulation extending from the bottom to the upper end of the heated zone and a double-walled cooling jacket of Inconel (inner tube) and stainless steel (outer tube) over the entire length. The annulus between shroud and cooling jacket is purged (after several cycles of evacuation) and then filled with stagnant argon at 0.22 MPa absolute. The annulus is connected to a flow- and pressure-controlled argon feeding system in order to keep the pressure constant at the target of 0.22 MPa and to prevent an access of steam to the annulus after shroud failure. The 6.7-mm annulus of the cooling jacket is cooled by argon flow from the upper end of the heated zone to the bottom of the bundle and by water in the upper electrode zone. Both the absence of ZrO_2 insulation above the heated region and the water cooling are to avoid too high temperatures of the bundle in that region.

The off-gas including Ar, H_2 and steam is analysed by a state-of-the-art mass spectrometer Balzers "GAM300" located at the off-gas pipe ~2.66 m downstream the test section. The mass spectrometer allows also to indicate the failure of rod simulators by detection of Kr release.

The test bundle, shroud, and cooling jacket are extensively equipped with sheathed thermocouples at different elevations with an axial step of 100 mm. There are 40 high-temperature (W/Re) thermocouples in the upper hot bundle region (elevations between 650 and 1350 mm) and 32 low-temperature (NiCr/Ni) thermocouples in the lower "cold" bundle region (bundle and shroud thermocouples between –250 and 550 mm). At elevations 950 and 850 mm there are two centreline high-temperature thermocouples in the central rod, which are protected from oxidising influence of the steam. Two thermocouples isolated from steam are installed at the same elevations inside the corner rods A and C. Other bundle thermocouples are attached to the outer surface of the rod cladding. The shroud thermocouples are mounted at the outer surface of Zircaloy-4 shroud. Additionally the test section incorporates pressure gauges, flow meters, and a water level detector. Further details of the QUENCH facility and operation are given by Schanz et al [12].

2.2 QUENCH-16 test conduct and main results

The test was performed with a bundle similar to that of used in QUENCH-10 test with Zircaloy-4 cladding. The experience of the QUENCH-10 test provided very valuable information for test preparation and for this reason the QUENCH-16 scenario was specified with the modification of QUENCH-10 scenario. Two important changes were considered in the QUENCH-16 scenario:

- Pre-oxidation period was shortened compared to QUENCH-10 to produce thinner (100-200 µm instead of 500 µm) oxide scale on the cladding. The oxidation temperature and power was kept similar to QUENCH-10.
- The air ingress phase lasted longer and the maximum temperature was lower than in QUENCH-10. During the specification of the test conditions it was emphasized that oxygen starvation should be established in the upper part of the bundle. The power and the air flow rate could be reduced and the argon flow rate increased if it proved necessary to reach this condition. It was proposed to seek an average heat-up rate in this phase between 0.1-0.2 K/s.

The QUENCH-16 test conduct comprised the following tests phases summarised in Table I.

Table I: Outline of test conduct.

	Heat-up to peak cladding temperature T_{pct}=873 K
Phase I	Stabilization at 873 K; facility checks
Phase II	Heat-up with 0.1-0.4 K/s to 1300 K during 2300 s
Phase III	Pre-oxidation of the test bundle in a flow of 3.3 g/s superheated steam and 3 g/s argon during 4000 s at temperature increased from 1300 K to 1430 K
Phase IV	Intermediate cooling from 1430 K to 1000 K during 1000 s in the same flow of steam and argon.
Phase V	Air ingress and transient heat-up from 1000 K to 1873 K with slow heating rate of 0.2 K/s in a flow of 0.2 g/s of air for 4040 s. Total oxygen consumption during 835 s before end of this phase.
Phase VI	Quenching of the bundle by a flow of 50 g/s of water. Temperature escalation to 2420 K with intensive hydrogen release.

Figure 3 illustrates the phases of test performance. In pre-oxidation phase and following slow cooling phase the claddings were oxidised in superheated steam (3.3 g/s). Maximal thickness of the ZrO_2 layer for withdrawn rod B was 130 µm. In the subsequent air ingress phase, which lasted 4035 s, the steam flow was replaced by 0.2 g/s of air. The change in flow conditions had the immediate effect of reducing the heat transfer so that the temperatures began to rise again. After some time measurements demonstrated gradually an increasing consumption of oxygen, accompanied by acceleration of the temperature increase at certain locations. The faster increase was most marked at the mid elevations of the bundle. Oxygen was completely consumed at about 3200 s after beginning of air ingress (Figure 4). Shortly before that time, partial consumption of the nitrogen was first observed, indicating local oxygen starvation which promoted the onset of nitriding. Following this, the temperature continued to increase until water injection was initiated when the maximum observed temperature was ca. 1873 K. Thus there was a period of about 835 s complete oxygen consumption and hence starvation in at least part of the bundle. The total uptakes of oxygen and nitrogen were about 58 and 29 g, respectively. The generally limited rate of temperature increase was the result of a rather low air flow rate, probably not untypical of reactor or spent fuel pool conditions.

The reflood was initiated by injecting 50 g/s of water, which value was reached in 25 s after beginning of water injection and thereafter was stable. Almost immediately after the start of reflood there was a temperature excursion in the mid to upper regions of the bundle (500 to 1400 mm), leading to maximum measured temperatures of about 2420 K. Cooling was established at the hottest location ca. 70 s after the start of injection, but was delayed further at other locations. Reflood progressed rather slowly, perhaps due to the high temperatures and partial degradation, and final quench was achieved after about 500 s. In line with the temperature escalations, a significant quantity of hydrogen was generated during the reflood (128 g). There are also indications of nitrogen release during the quench phase (24 g from 29 g consumed during oxygen starvation period).

Investigations of corner rod D, withdrawn at the end of the air ingress phase, showed significant spalling of oxide scales and intensive nitride formation between elevations 300 and 900 mm. Therefore, the oxide layer, formed during the preoxidation phase, had no protection function in this bundle region, characterized by oxygen starvation conditions.

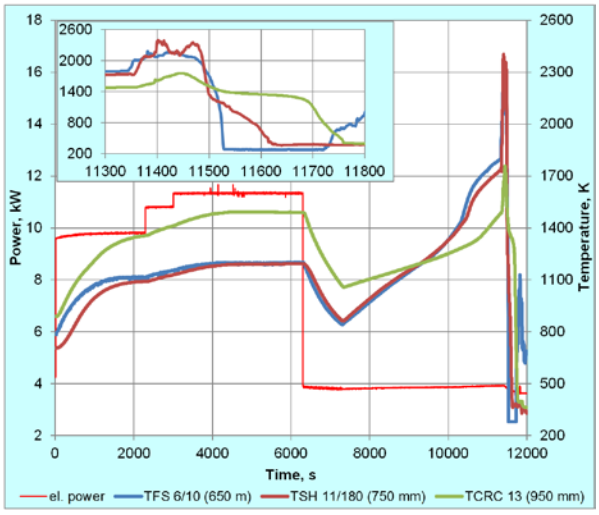

Figure 3. QUENCH-16 test conduct showing electric power input and selected temperatures.

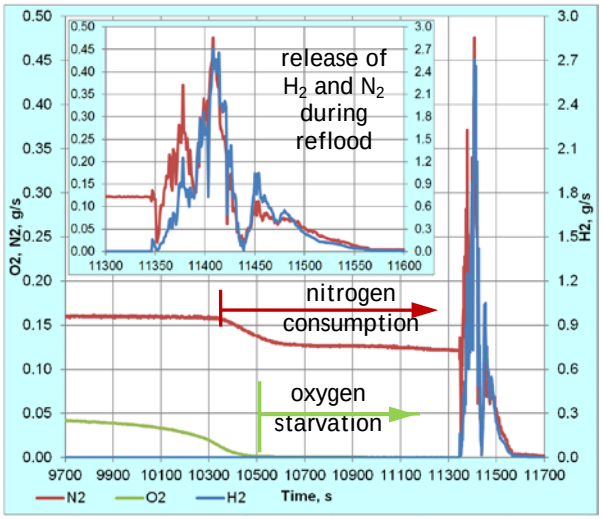

Figure 4. QUENCH-16 mass spectrometer analysis of off-gas.

The videoscope inspection at positions of withdrawn corner rods shows an intensive degradation of the oxide layer with partial spalling at bundle elevations between 450 and 850 mm (Figure 5). Coloured outer oxide scales (perhaps due to small nitride traces) at outer surface of claddings were observed at elevations between 750 and 900 mm (Figure 6). The reflood oxidation and degradation were not specifically planned and was not expected, but an outcome of the experiment that could not necessarily be prevented.

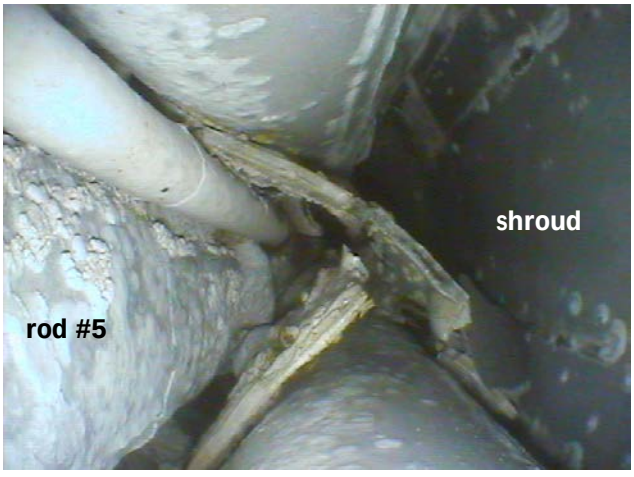

Figure 5. Post-test videoscope inspection (front view) at bundle elevation 550 mm.

Figure 6. Post-test videoscope inspection (side view) at bundle elevation 790 mm.

After videoscope investigations the bundle was filled with the epoxy resin, which was hardened during two weeks. Then the bundle was cut at different elevation and corresponding cross sections were grinded and polished. Metallographic investigation of cross sections between 300 and 500 mm showed frozen partially oxidised melt (Figure 7), relocated from upper elevations 500 – 800 mm, which could have been the main source of hydrogen during reflood. At elevations 800 – 900 mm only local melt between pellet and outer oxide layer was observed (Figure 8). No melt was formed at elevations above 900 mm. The image analyses of the melt enables estimation of the influence of melt oxidation

on the hydrogen production: this source contributes about 20% of hydrogen release during reflood. The EDX analyse showed that more than 50% of melt was produced by shroud. However the cladding melt oxidation degree was higher in comparison to the shroud melt – probably due to higher temperatures inside the bundle.

Figure 7. Bundle cross section at 430 mm: frozen melt relocated from upper elevations

Figure 8. Bundle cross section at 830 mm: minor melting of some cladding segments

A very intensive nitride formation was observed at elevations 350 – 550 mm (Figures 9 and 10). The upper oxide scales above nitrides have a porous structure due to re-oxidation of nitrides during reflood (Figure 10). At elevations above 550 mm only some nitride traces at the boundary between inner dense and spalled outer porous oxide scales were observed.

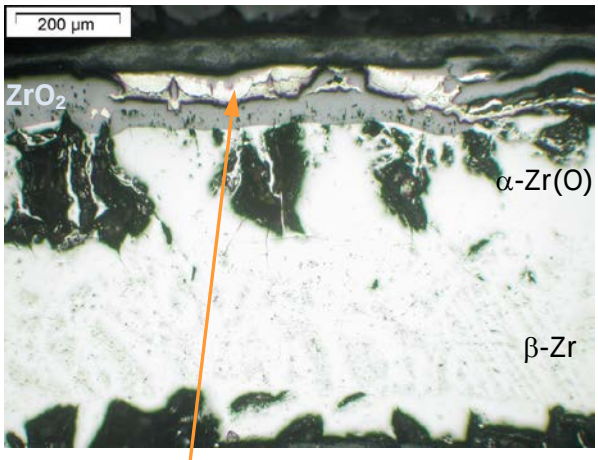

Figure 9. Bundle elevation 350 mm, cladding of rod #5: nitrides between two oxide layers

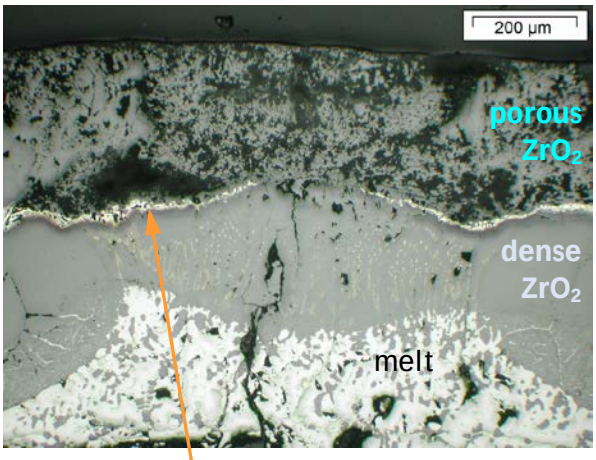

Figure 10. Bundle elevation 550 mm, cladding of rod #9: nitrides between inner dense and outer porous oxide layers

The observed nitrogen consumption and the presence of nitride at many locations suggest that its formation is not prevented by the prior formation of an oxide layer. If the oxide layer is thin enough it can be dissolved completely during the starvation phase with development of very thick α-Zr(O) layer, in other cases the α-Zr(O) precipitates are formed

directly inside thick oxide layer [18]. The availability of oxygen in cladding (α-Zr(O) formation) accelerates dramatically the nitriding process with formation of very porous nitride layer [6]. A noticeably thick oxide sub-layer was formed under nitride layer during the reflood phase due to intensive steam penetration through the porous outer nitride layer. First estimations of ongoing metallographic measurements showed that more than 50% of hydrogen released during the reflood are connected with this oxidation mechanism. More details will be given in the experimental KIT report.

3 PRE-TEST ANALYTICAL SUPPORT

Pre-test analytical support was performed by GRS, EDF and PSI, respectively using the simulation tools ATHLET-CD, MAAP-4.07(EDF), SCDAPSim/Mod3.5 and MELCOR V1.8.6. The analyses were performed specifically to identify a test protocol that would result in achievement of the test objectives:

Pre-oxidation at a maximum temperature of ca. 1200 C (1473K), resulting in a maximum oxide layer thickness 100 - 200 µm.

Cooling of the bundle to ca. 850 C (1123 K) prior to switching from steam to air inlet flow.

Gradually increasing temperatures and oxidation rate until all of the oxygen is consumed.

A long oxygen starvation period target of 15 mins (900 s) before temperatures reach 1550 C (1823 K) before reflood.

Ideally, a scenario would be identified in which all the simulations would predict the meeting of these objectives.

The most challenging aspect of the planning was the fourth objective. A low air flow rate was required to achieve the starvation, but a low flow would imply low convective heat transfer from the heater rods and hence increasing temperatures. A range of possible power and argon/air flow rates were analysed, covering the range

Preoxidation

Power: ca. 10 kW for 5000 s (to achieve 100 – 200 µm ZrO_2), then reduce

Flow rate: 3 g/s steam; 3 g/s Ar

Air phase

Power: 4 – 7 kW

Flow rate: 0.1 – 0.5 g/s air; 1-3 g/s Ar

It was decided to focus on the following sequence. Terminate the preoxidation by reducing the power to 4 kW, cool down for 1000 s, and conduct the air phase with 0.2 g/s air and 3 g/s argon flow, reflood at T_{max} = 1823 s. However, the oxygen concentration would be only about 5 vol %. Supporting air oxidation SETs by KIT showed a strong reduction in oxidation rate at low air concentrations. It was accordingly decided reduce the argon flow to 1 g/s to reduce this impact.

3.1 ATHLET-CD analysis

In the following chapter a short overview over the air ingress model implemented in ATHLET-CD and its use for previous simulations is given. The results of the analytical support to QUENCH-16 are presented in a brief description.

3.1.1 Air oxidation model of ATHLET-CD

The ATHLET-CD version 2.2b, which was used for the pre-test analytical support of the QUENCH-16 test, provides several correlations to calculate the air oxidation reaction rate R_i (Figure 11) [19]. Similar as the steam oxidation the reaction starts with parabolic kinetics with $dm'/dt = R_i(T)/m'$, where m' is the mass of oxidized zirconium per surface area in kg/m^2. At a certain oxide layer thickness, defined by input data (standard value ROXLMA=250 µm), a transition to linear kinetics is made, with the effect that a further increase of oxide mass is not considered in m' on the right side of the above equation to simulate the effects of cracking and breakaway observed in the experiments.

The reaction rate R_i is an Arrhenius type equation of the form $R_i=A_i \cdot e^{(-Ei/T)} \cdot g(p_{O2}) \cdot F_{lim,O2}$, where i corresponds to the input value of the oxidation correlation IOXAIR=1,..8. The factor $g(p_{O2})$, which is defined in the range $0 \le g(p_{O2}) \le 1$, considers starvation of oxygen. It is a polynomial for $f_p=(p_{O2}/p)/x_{lim}$, where p_{O2} is the partial pressure of oxygen, p is the total pressure of the steam/gas mixture and x_{lim} is the upper limit of p_{O2}/p to start the reduction to values below 1. The definition of $g(p_{O2})$ as a polynomial provides a smooth and steady interruption or activation of the air oxidation reaction during a transition into or out of an oxygen starvation phase, respectively. The recommended value to initiate the reduction is $x_{lim}=0.05$ (input value OXO2LIM). The input value $F_{lim,O2}$ was originally intended as a preliminary compensation for the previously unavailable nitride formation model; now it is used to consider geometric effects (shroud: FLIMOX=0.1, grids: FLIMOX=0, for rods: FLIMOX=1) corresponding to the experimental results which would overestimate the air reaction for components with other geometries using the empirical values mainly derived for rods.

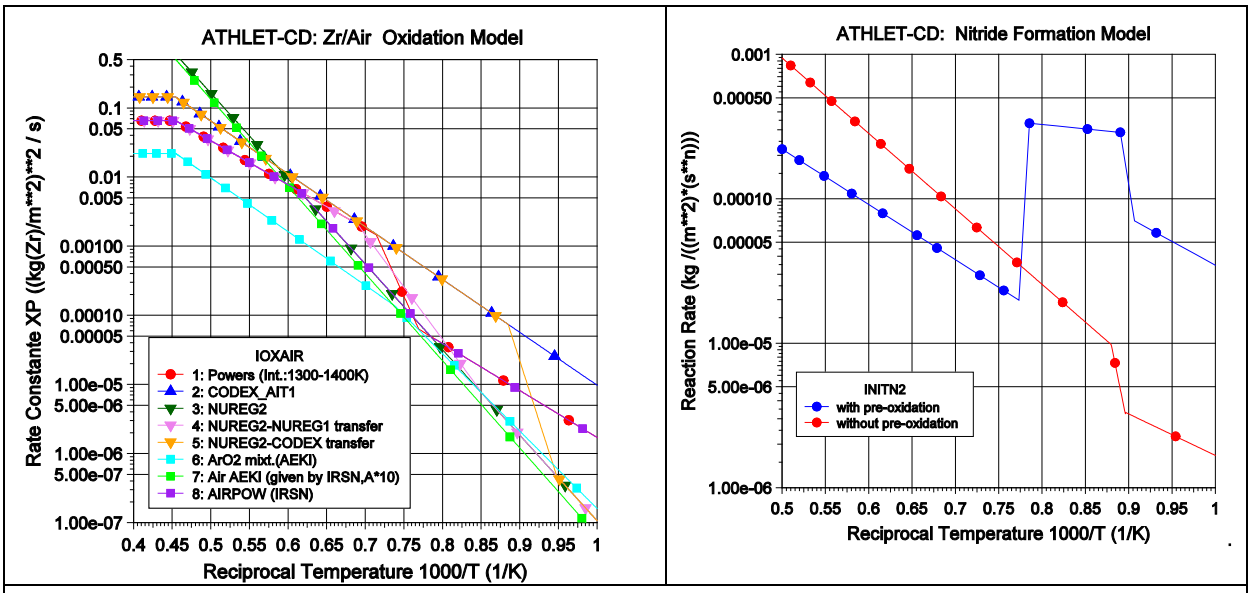

Figure 11: Available correlations for Zr/air oxidation and nitride formation in ATHLET-CD

For the parametric study of these pre-test calculations a test version of the nitride formation model was adopted, where a first approach is formulated to consider also the nitrogen reaction. Again, the mass gain is formulated as a function of the reaction rate, a time depending value and the free surface for the reaction: $\Delta m=R_i(T) \cdot t^{n_i} \cdot A_{rod}$. The reaction rate R_i is also expressed as an Arrhenius function including comparable parameters A_i and

E_i for nitrogen. By using the method of least squares the parameters for the empirical correlations are determined on the basis of single effect tests performed at KIT, Germany. For the determination of the parameters it is also necessary to distinguish between cladding which is pre-oxidized or not, therefore now 2 different correlations for the reaction rate are available [20] (Figure 11).

As the formation of nitride is observed only in situations when oxygen starvation occurs, the calculated reaction rate increases from 0 to the full value when the partial pressure of oxygen decreases between $10^{-2} \geq p_{O2}/p \geq 10^{-3}$.

The exothermal energy of the zirconia and nitride formation is considered as heat source of the cladding and the consumed oxygen and nitrogen are treated as mass sink of the fluid-dynamic system.

3.1.2 Verification of ATHLET-CD for air ingress and input model for QUENCH-16

The above described modelling of air ingress was tested and verified with the following simulations:

- Post-test calculation of QUENCH-10
  (comparison of the different options for the oxidation reaction)
- Post-test calculation of CODEX-AIT1
  (examination of the model in particular with regard to shroud and grid oxidation in comparison with cladding oxidation)
- Pre- and post-test calculation of PARAMETER-SF4
  (application of new model to consider ZrN formation)

Based on the same nodalization as used for QUENCH-10 (Figure 12) the options and input parameters which resulted in best agreement during a rerun of QUENCH-10 were used for the pre-test support to QUENCH-16.

3.1.3 Results of analytical support for QUENCH-16

For the originally proposed conditions [21] with a power increase from 10 to 11 kW during the pre-oxidation phase at a steam flow rate of 3 g/s the resulting temperature plateau was higher than intended (1500 K instead of 1450 K) and the oxide layer thickness prior to start of air ingress was 250 µm and therefore above the aimed values of 100-200 µm. The argon flow rate of 3 g/s and air flow rate of 0.25 g/s together with a power of 7 kW during the air ingress phase lead to a too fast temperature increase with maximum temperatures above 1823 K within half the time intended for air ingress (80-100 min). Therefore the boundary conditions were changed to achieve the defined test objectives with a lower oxide layer thickness before air injection and a time period of about 100 min. to reach the final temperature maximum of 1823 K at the end of the air ingress phase. These conditions were met with a reduced power (9-10 kW during pre-oxidation, 4.75 kW during air ingress). As the starvation was shorter than intended, an additional reduction of air flow rate to 0.2 g/s was recommended with a further reduction of power to 2.5 kW during the starvation period. With these options no further escalation at start of quenching was calculated.

The updated specification [22] recommended a power of 10 kW with 3 g/s steam flow during the pre-oxidation phase, for which the simulation resulted in the desired plateau temperatures of ~1450 K and a maximum oxide layer thickness of 190 µm before air ingress. During the intermediate cooling and air ingress phase a power of 4 kW was suggested, with an argon flow rate of 3 g/s and an air flow of 0.2 g/s. These boundary conditions led to the intended scenario in which the temperature increase was slow enough but the starvation was short (470 s) and restricted to the upper bundle elevations.

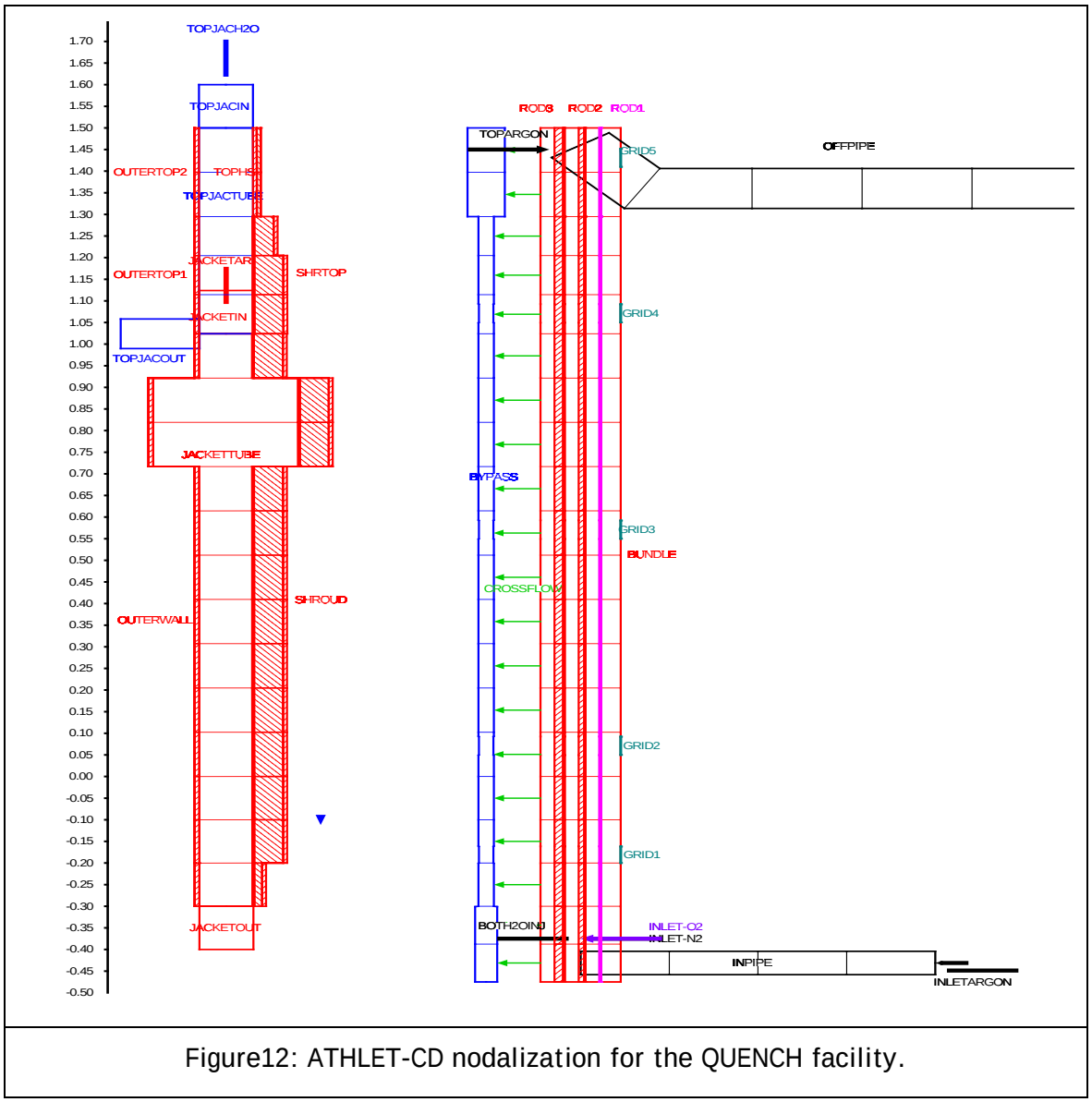

Figure12: ATHLET-CD nodalization for the QUENCH facility.

The alternative simulation with a reduced argon flow rate of only 1 g/s at start of air ingress, as used later in the experiment, also led to a slow heat up (Figure 13). After a time period of 3420 s upon start of air ingress quenching was initiated at 9420s. This simulation with the lower argon flow rate showed that in this case an even more distinctive oxygen starvation would occur also at middle and lower bundle elevations over a period of ~ 15 minutes (8500 to 9420s: ~920 s) (Figure 14). However, both simulations did not predict the escalation which was observed in the test after start of flooding, therefore the hydrogen mass, which was 11 g after pre-oxidation increased only slightly during quenching.

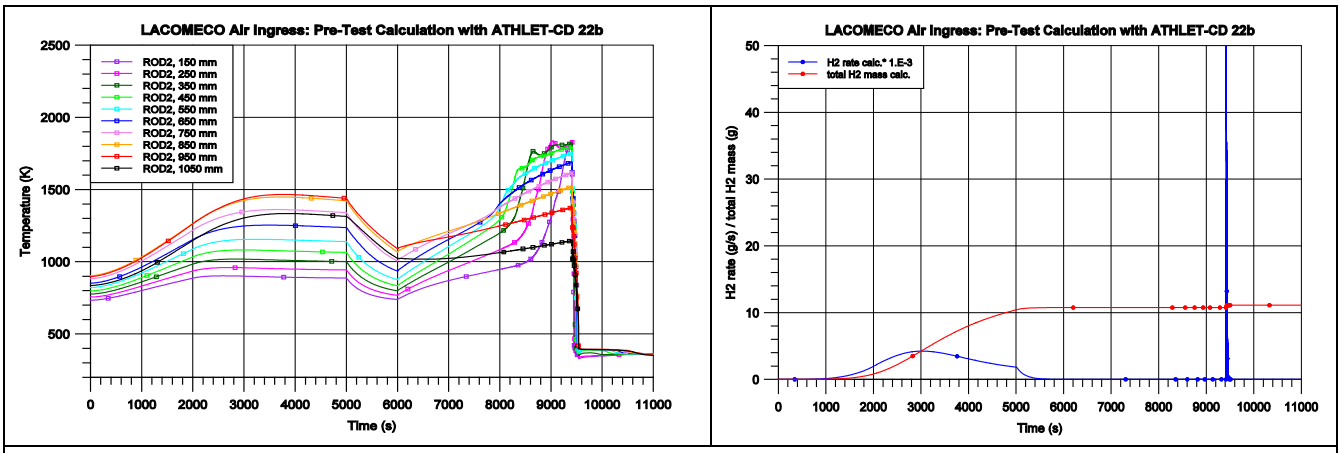

Figure 13: Fuel rod temperatures and hydrogen generation for simulation with G(argon)=1 g/s,

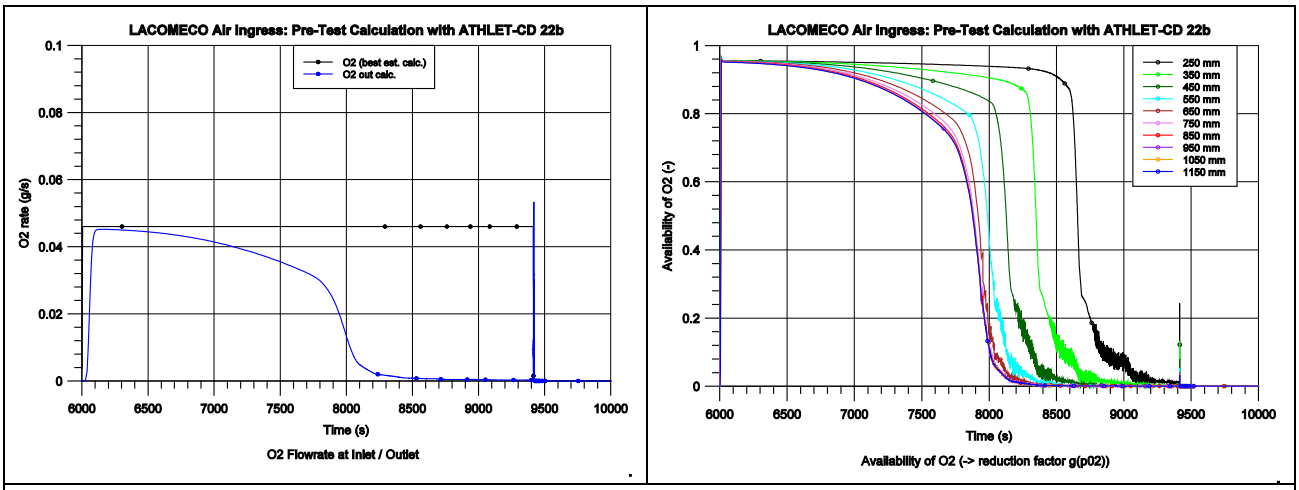

Figure 14: Starvation condition for simulation with G(argon)=1 g/s.

3.2 MAAP4-EDF analysis (EDF)

3.2.1 Air oxidation model in the EDF version of MAAP4.07

MAAP [23] is used to simulate severe accident transients. It was originally developed for the Industry Degraded Core Rulemaking (IDCOR) program in the early 1980s by Fauske and Associates, Inc. (FAI). At the completion of IDCOR, ownership of MAAP was transferred to the Electric Power Research Institute (EPRI), which is now in charge of improving the code and licensing it to utilities, vendors and research organizations. The current version of the code, called MAAP4.07, has no provision for modelling air ingress. Thus, it was modified by EDF to make it suitable for the present task.

Additions were implemented in the code to model the reaction of Zry-4 with air, essentially the oxygen part. Cladding weight gain correlations are converted in terms of an oxide thickness, representing oxide layer growth :

$$x^n = \frac{K_m(T).t}{\rho^n},$$

with ρ, zirconium density in $kg.m^{-3}$ and $K_m(T)$, in $kg_{(Zr)}{}^n.m^{-2n}.s^{-1}$, which corresponds to the law selected by the user and $n = 2$ for a parabolic law, 1 for a linear law and 0.5 for an accelerated law.

Several weight gain correlations are available [19] in this MAAP4.07 version, which can be selected by the user with a simple option choice. According to the currently available correlations and our previous studies, the NUREG correlations set [1] is considered as the reference law, although parabolic :

- for T < 1333 K : $K(T) = 10.5 \exp\left(\frac{-15630}{T}\right)$,
- for 1333 K ≤ T ≤ 1550 K : $K(T) = 25.11 * 10^4 \exp\left(\frac{-28485}{T}\right)$,
- for T > 1550 K : $K(T) = 50.4 \exp\left(\frac{-14634}{T}\right)$,

which are expressed in $kg_{(Zr)}^2.m^{-4}.s^{-1}$.
Finally, to optimize changes to the code for reactor applications with complex atmospheres, the effect of a steam/oxygen mixture is treated in the code. In MAAP4.07, it is possible to oxidize with both steam and oxygen:

- if there is enough zirconium, cladding oxidation is calculated with both gases, in accordance with their own oxidation kinetics,
- if there is little zirconium left, cladding oxidation is calculated in proportion to the gas mass flow rates,
- for a ratio of mass flow rates less than 10^{-6}, oxidation is calculated with the major component only.

3.2.2 Pre-test calculations with the EDF version of MAAP4.07

EDF participated in pre-test calculations to help to define the transient of the future QUENCH-16 experiment. To conduct these calculations, EDF had to take into account the different experimental needs.

A first set of pre-test calculations was performed according to the original proposal [21] within which adjustments of some experimental parameters were allowed: injected power, duration of the different steam and air oxidation plateaus and argon flow rates, to achieve the needed conditions presented in 1. These first calculations considered a transient with a pre-oxidation phase of about 5400 s under 3 g/s of steam and 3 g/s of argon, a cooldown of about 1000 s under the same atmosphere, an oxidation phase of about 5400 s under 0.2 g/s of air and a variation of argon from 7.5 to 10 g/s, a final quenching under 50 g/s of water. These conditions lead to an oxide layer of about 200 µm at the end of the cooldown and an oxygen starvation phase of about 500 s.

Following a review of results of the first calculations by the participants, a second set of calculations was performed based on the revised proposal [22] from which the final experiment specification was defined. In addition a sensitivity study on the argon flow rate (comparison of the case with 1 g/s of argon with the one with 3 g/s). During the pre-oxidation phase, about 19 g of hydrogen were produced and an oxide layer thickness of about 242 µm was formed. For the air phase, the temperature criterion of 1823 K was achieved after 2700 s for the case with 1 g/s of argon and after 3000 s for the case with 3 g/s. This temperature criterion leads to a reflood at ~8720 s in the first case and at ~9000 s for the second one. For the first case, oxygen starvation condition was achieved during 1150 s and during 1100 s for the second one. As shown by comparison of the Figure 15 (a, b) and 16, a longer oxygen starvation duration is thus established with 1 g/s of argon and in a larger part of the bundle. These observations are confirmed by the temperature evolution graph on the Figure 15: temperatures are higher in the middle part of the bundle with 1 g/s of argon. As oxygen is consumed at the top of the bundle (cf. Figure 15(a) and (b)), the exothermal oxidation occurs at lower elevations. The simulations results with MAAP support the experimental choice of 1 g/s of argon to achieve an appropriate starvation period.

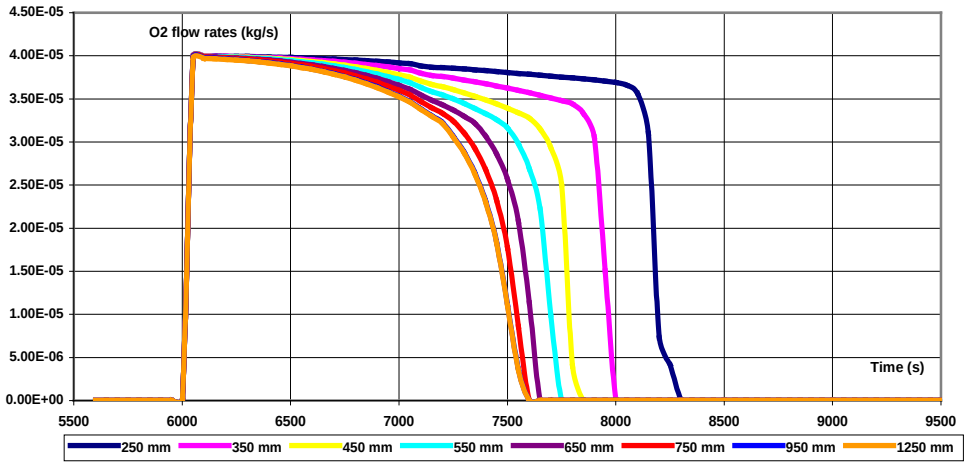

Figure 15(a): Oxygen flow rates evolution at different bundle heights for 1 g/s of argon.

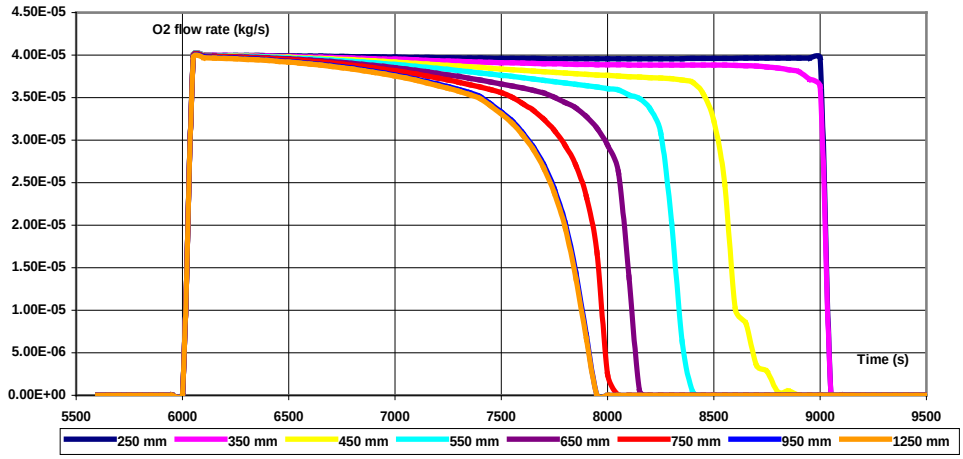

Figure 15(b): Oxygen flow rates evolution at different bundle heights for 3 g/s of argon.

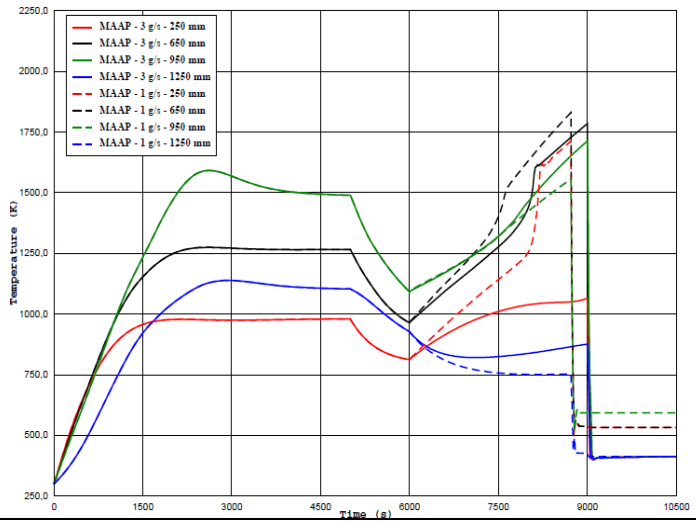

Figure 16: Temperature evolution for the cases with 3 g/s (solid lines) and 1g/s of argon (dashed lines) at 250 mm, 650 mm, 950 mm and 1250 mm bundle heights.

3.3 MELCOR and SCDAPSIM analysis (PSI)

Both MELCOR and various SCDAP-based code versions have been used at PSI to provide planning support and post-test analyses of QUENCH experiments [24], [25]. Versions of SCDAP have been most widely used in the past by virtue of the more complete hydraulic modelling, but MELCOR was the preferred choice for Q-10 since SCDAP did not at the time furnish any treatment of air oxidation, whereas MELCOR contains a separate correlation for the air oxidation kinetics, and treats oxygen as a chemically active species. Post-test analysis with MELCOR and the findings of experimental programmes in the following years revealed major shortcomings in the MELCOR kinetics correlation. In particular the possible transition to breakaway kinetics is not represented. A new model has therefore been developed [26].

The new model employs a choice of kinetic parameters that are the same as in existing correlations [27], [28], [29], [30]. The default model for steam is Cathcart-Pawel/Urbanic Heidrick, as in the standard SCDAP, while the default for oxygen is Uetsuka –Hofmann at low to moderate temperatures and Cathcart-Pawel/Urbanic Heidrick at higher temperature outside the range of the Uetsuka data. The key feature of the model is a temperature-dependent criterion for the onset of transition to breakaway oxidation, the fully developed breakaway state, and the transition period within which the kinetics changes from parabolic to linear. The criterion is largely determined from results of SETs performed by KIT [31] and IRSN [19]. Implementation in MELCOR is currently in progress, but a new version of SCDAPSIM containing the model has gave good results in a recent analysis of air ingress experiment PARAMETER-SF4 [32]. Unlike ATHLET, the air oxidation model in SCDAPSIM considers only oxygen as the active species. Nitride formation is not (at present) represented, and nitrogen effectively acts as a catalyst by promoting breakaway.

Calculations were performed with both codes, using the new model in SCDAPSIM with breakaway oxidation enabled for air but disabled for steam, and using a variety of parabolic correlations (i.e. no breakaway) with MELCOR. The new model was not implemented in MELCOR at the time of the analysis and the default Urbanic-Heidrick correlation for steam was used. The first set of calculations concentrated mainly on a test protocol 3 g/s argon. Although both codes indicated that the test objectives, in particular the 15 minute target for oxygen starvation would be met with the originally considered flow rates, 3 g/s argon and 0.3 g/s air, there are disadvantages of such a low air concentration. Attention therefore focussed on a reduced argon flow of 1 g/s.

Figure 17 shows the SCDAPSIM calculated effect of the different candidate air and argon flow rates on the heat up and time window between the onset of starvation (indicated by dash lines) and reflood (the temperature drops sharply). The starvation period depends strongly on the air flow rate, and is about 150 s with 0.5 g/s air (either 1 or 3 g/s argon), about 1500 s with 0.2 g/s air + 1 g/s argon, and 3300 s with 0.2 g/s air + 3 g/s argon. Figure 18 shows the oxygen consumption which starts very slowly before increasing sharply.

Calculations with both codes indicated that the target starvation period would be achieved with 0.2 g/s air and 1 g/s argon. Sensitivity studies suggested that this result was robust to uncertainties in the oxidation kinetics. Counterpart calculations with MELCOR yielded a similar conclusion.

The final base case was performed with SCDAPSIM. The thermal evolution at the different elevations, Figure 19, shows the temperature increase to be predicted first at the current maximum temperature location towards the top of the bundle and then shift downward following the location of complete consumption, shown in Figure 20.

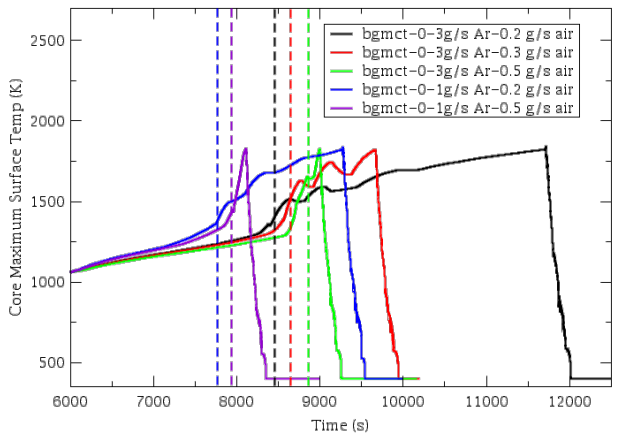

Figure 17: Predicted effect of Ar and air flow rate on thermal response.

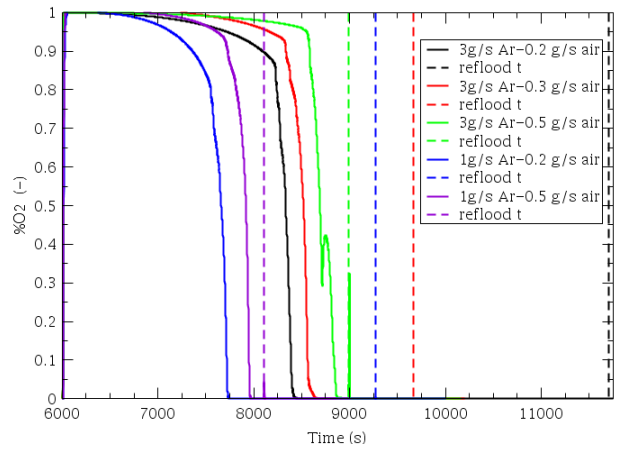

Figure 18: Predicted effect of Ar and air flow rate on oxygen consumption.

Slightly surprisingly the base case model did not predict breakaway during the air phase - the criterion for breakaway was nearly reached but not quite. However, breakaway was calculated in some of the sensitivity cases. The non-smooth behaviour concerning the oxygen consumption (Figure 19) is an anomaly due to a mismatch in the way the diffusion limit is applied on the different components and should be rectified when the code version is formally released.

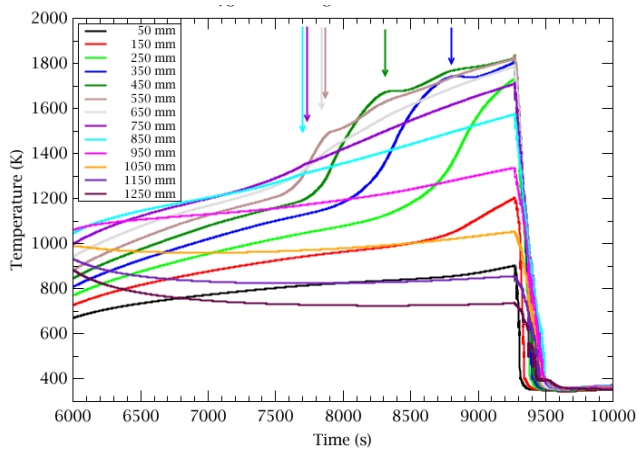

Figure 19: Predicted thermal escalation during QUENCH-16 air phase, indicating starvation progression (1.0 + 0.2 g/s Ar + air).

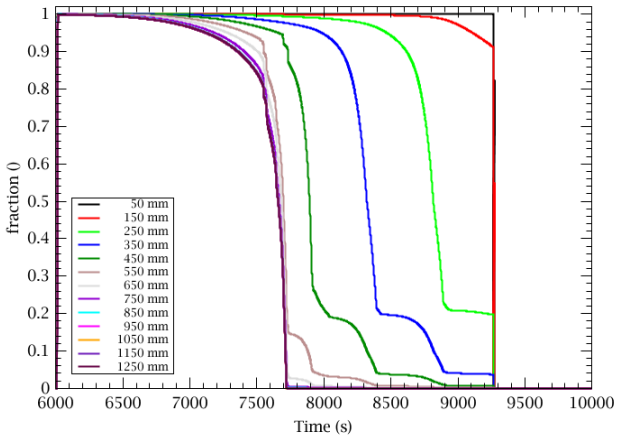

Figure 20: Predicted oxygen consumption during QUENCH-16 air phase (1.0 + 0.2 g/s Ar + air).

3.4 Summary of results

It should be made clear that the pre-test analyses were not aimed at code or model assessment, nor interpreting the observed transient behaviour. Comparison with the data is qualitatively interesting but differences between the assumed and experimental conditions mean that any quantitative comparisons are of dubious value.

The results all indicated that 1 g/s or 3 g/s argon + 0.2 g/s air would provide more than 900 s starvation period, while an increased air flow or reduced argon flow would reduce the starvation period, Indeed, not all the models at higher air flow rates (0.3 or 0.5 g/s)

predicted the full 900 s oxygen starvation. An argon flow of 1 g/s was chosen to avoid excessive dilution of the oxygen. The results of the finalised test conditions are summarised in Table II. In fact reflood was initiated in the experiment at 1873 K after a starvation period of 835 s.

Table II: Predicted main parameters and comparison with experiment.

Partner (Code)	PSI (SCDAPSIM)	PSI (MELCOR1.8.6)	GRS (ATHLET-CD)	EDF (MAAP 4.07)	Experiment
Heat-up	0-5000 s	0-5000 s	0-5000 s	0-5000 s	0 – 6300 s
Pre-oxidation					
Power	10 kW	10 kW	10 kW	10 kW	10 – 11.5 kW
Ar + steam	3 g/s + 3 g/s	3 g/s + 3 g/s	3 g/s + 3 g/s	3 g/s + 3 g/s	3 + 3.3 g/s
Tmax (5000 s)	1440 K	1422 K	1440 K	1480 K	1489 K
Cooldown	5000-6000 s	5000-6000 s	5000-6000 s	5000-6000 s	6300 – 7300 s
Power	4.0 kW	4.0 kW	4.0 kW	4.0 kW	4.0 kW
Ar + steam	3 g/s + 3 g/s	3 g/s + 3 g/s	3 g/s + 3 g/s	3 g/s + 3 g/s	3 + 3.3 g/s
Tmax (6000 s)	1061 K	1098 K	1090 K	1100 K	1067 K
Air phase	6000 - 9260 s	6000 – 8350 s	6000-9420 s	6000-8700 s	7300 – 11335 s
Power	4.0 kW	4.0 kW	4.0 kW	4.0 kW	4.0 kW
Ar + air	1 g/s + 0.2 g/s	1 g/s + 0.2 g/s	1 g/s + 0.2 g/s	1 g/s + 0.2 g/s	1 g/s + 0.2 g/s
Quench(temp)	9260 s (1823 K)	8350 s (1823 K)	9420 s (1823 K)	8750 s (1830 K)	11135 s (1883 K)
Fast refill + 50 g/s water	4 kW	4 kW	0 kW	0 kW	4 kW
H2 mass,	13 g	15 g	11 g	19 g	14 g
Max. oxide after pre-oxidation	186 /µm	190 µm	190 µm	ca. 242 µm	133 µm
Duration air phase/ starvation	3260 s 1540 s	2350 s 1660 s	3420 s 920 s	2750 s 1150 s	4035 s 835 s
H2 mass (refl)	2 g	16 g	1 g	1 g	128 g
Remarks	ca. 3000 s starvation if 3 g/s Ar no influence of 0/4 kW during quench		ca. 470 s starvation if 3 g/s Ar ZrN model would increase starvation time	ca. 1100 s starvation if 3 g/s Ar	

4 CONCLUSIONS AND FUTURE PLANS

The successful conduct of QUENCH-16 yielded valuable data on air oxidation at low air flow rate, in particular the transition to rapid oxidation by oxygen, the progress of the starvation front, and the nitrogen interaction. The results will support further assessment and development of the air oxidation models. The contrast with QUENCH-10 regarding amount of pre-oxidation and duration of oxygen starvation implies a large addition to the database on air ingress.

There was evidence of nitriding in both the oxygen-starved and non-starved regions and spalling of both oxide and nitride layers. The results strengthen the case for representing the Zr-nitrogen reaction in the analysis codes, currently not included in most codes.

The strong reflood excursion results in maximum temperatures well above the metallic Zircaloy melting point and was accompanied by relocation and oxidation of metallic melt. The mechanism that drove the excursion is not yet conclusively identified, but may have been a result of either or both of (i) damage to the oxide layer caused by the nitrogen and (ii) diffusion of oxygen into the underlying alpha-phase metallic during the starvation period.

Achievement of the desired long period of oxygen starvation was facilitated by a careful specification of the test conditions, based on planning calculations by GRS, EDF and PSI using different simulation tools, from which the results indicated a consensus on the test protocol that was finally chosen. The preoxidation thickness and hydrogen production were within the target band and comparable with the predicted values. The starvation period also lay within the range of predictions though slightly below the target of 900 s.

The biggest difference in the experiment outcome in comparison with QUENCH-10 was the large oxidation excursion during reflood. None of the calculations predicted the excursion. The models for air oxidation are not yet complete enough to describe reliably the processes that are likely to have been instrumental in promoting the excursion. This topic is identified for ongoing analysis.

The other main differences between prediction and experiment result from minor differences between the nominal and actual conditions, and mainly affect event timings.

Post-test analyses of the results are underway among the SARNET-2 WP5 participants, including those involved in the planning support. There are plans to perform a benchmark exercise within JPA3, covering the air ingress tests QUENCH-10 and -16 in order to benefit fully from the experimental results. It is anticipated that the analyses will proceed hand-in-hand with model developments.

ACKNOWLEDGEMENTS

The LACOMECO programme is performed by KIT with financial support from the HGF Programme NUKLEAR and the European Commission. Technical support is provided by institutes with the European Economic Area.

The development and validation of the code ATHLET-CD are sponsored by the German Federal Ministry of Economics and Technology (BMWi). PSI acknowledges financial support of ENSI, the Swiss nuclear regulatory organisation.

REFERENCES

[1] D.A. Powers, L.N. Kmetyk and R.C. Schmidt, "A Review of The Technical Issues of Air Ingression During Severe Reactor Accidents". Technical Report, NUREG/CR-6218, Sandia National Laboratories, 1994.

[2] J.-C. Micaelli et al., SARNET - A European Cooperative Effort on LWR Severe Accident Research, Revue Générale Nucléiare 2006, no. 1, January -February 2006.

[3] Clément, B., 2002. Towards Reducing the Uncertainties on Source Term Evaluations: an IRSN/CEA/EDF R&D Programme. Proc. EUROSAFE Forum, Berlin, 4-5 November 2005.

[4] Clément, B. and Zeyen, R., 2005. The Phebus Fission Product and Source Term International Programmes. Proc. Int. Conf. on Nuclear Energy in New Europe 2005, Bled, Slovenia, 5-8 September.

[5] Steinbrueck, M., 2008. Oxidation of Zirconium Alloys in Oxygen at High Temperatures up to 1600 °C. Oxidation of Metals, 70, 317-329.

[6] Steinbrueck, M., 2009. "Prototypical Experiments Relating to Air Oxidation of Zircaloy-4 at High Temperatures". Journal of Nuclear Materials 392, 531–544.

[7] L. Matus, N. Vér, M. Kunstár, M. Horváth, A. Pintér, Z. Hózer, "Summary of separate effect tests with E110 and Zircaloy-4 in high temperature air, oxygen and nitrogen, AEKI-FL-2008-401-04/01 (2008).

[8] Natesan, K. and Soppet, W. K., 2004. "Air Oxidation Kinetics for Zr-based Alloys". USNRC NUREG/CR-5846, ANL-03/32.

[9] OECD/NEA, Agreement on the OECD-NEA SFP Project: An Experimental Programme and Related Analyses for the Characterization of Hydraulic and Ignition Phenomena of Prototypic Water Reactor Fuel Assemblies, January 2009.

[10] Z. Hózer, P. Windberg, I. Nagy, L. Maróti, L. Matus, M. Horváth, A. Pintér, M. Balaskó, A. Czitrovszky, P. Jani: "Interaction of failed fuel rods under air ingress conditions", Nucl. Technology, 141, p. 244 (2003).

[11] J. Stuckert, J. Birchley, C. Homann, S. Horn, Z. Hozer, A. Miassoedov, J. Moch, G. Schanz, L. Sepold, U. Stegmaier, L. Steinbock, M. Steinbrueck, "Main results of the bundle test QUENCH-10 on air ingress". 10th International QUENCH Workshop, Karlsruhe, October 26-28, 2004.

[12] G. Schanz, M. Heck, Z. Hozer, L. Matus, I. Nagy, L. Sepold, U. Stegmaier, M. Steinbrueck, H. Steiner, J. Stuckert, P. Windberg, "Results of the QUENCH-10 experiment on air ingress". Scientific Report, FZKA-7087, SAM-LACOMERA-D09, Karlsruhe, Mai 2006. http://bibliothek.fzk.de/zb/berichte/FZKA7087.pdf

[13] Kisselev, A., Strizhov, V. and Vasiliev, A. 2010. "Application of Thermal Hydraulic and Severe Accident Code SOCRAT/V2 to Bottom Water Reflood Experiment PARAMETER-SF4", Proc. Nuclear Energy in New Europe 2010, 6-9 September 2010, Portorož, Slovenia.

[14] Z. Hozer, "QUENCH Test with Slow Oxidation in Air", Proposal for an Experiment within the LACOMECO Project (2010).

[15] A. Miassoedov: "LACOMECO project within the 7th EU FWP large scale experiments on core degradation, melt retention and containment behaviour", Proceedings of the 15th International QUENCH Workshop, Karlsruhe, November 3-5, 2009. CD-ROM, ISBN 978-3-923704-71-2.

[16] A. Miassoedov et al., "LACOMECO and PLINIUS experimental platforms at KIT and CEA". 4th European Review Meeting on Severe Accidents Research (ERMSAR-2010), Bologna. May 11-12, 2010.
http://www.sar-net.eu/sites/default/files/Paper-S3-4.pdf

[17] A. Miassoedov and D. Bottomley, "LACOMECO-MANAG-M02 Summary of the 1st User Selection Panel Meeting", Bratislava, Slovakia, July 8, 2010.

[18] J. Stuckert, and M. Veshchunov, "Behaviour of Oxide Layer of Zirconium-Based Fuel Rod Cladding under Steam Starvation Conditions", Wissenschaftliche Berichte, FZKA-7373, Karlsruhe, April 2008.
http://bibliothek.fzk.de/zb/berichte/FZKA7373.pdf

[19] O. Coindreau, et al., "Modelling of accelerated cladding degradation in air for severe accident codes", Paper No S.2.4 – Session Corium Issues, The 3rd European Review Meeting on Severe Accident Research (ERMSAR 2008), Nesseber, Bulgaria, September 2008.

[20] T. Hollands, C. Bals, H. Austregesilo, W. Luther, "Simulation of the air ingress experiment PARAMETER-SF4 using ATHLET-CD", NURETH-14, Toronto, Canada, September 25-29, 2011.

[21] Z. Hózer, "Air_ingress_scenario.doc", communication from February, 25, 2011.

[22] M. Steinbrueck, "QUENCH-16, updated specification", e-mail from April, 29, 2011.

[23] F.Rahn, "Technical Foundation of Reactor Safety - Knowledge Base for Resolving Severe Accident Issues, Technical Report", 1020497, EPRI, 2010.

[24] J. Birchley, T. Haste, C. Homann and W. Hering, "Pre-Test Analytical Support for Experiments QUENCH-10, -11 and -12", Paper 812, Proc. Conf. Nuclear Energy in New Europe 2006, Porteroz, Slovenia.

[25] J. Birchley and J. Stuckert, "Analysis of QUENCH-ACM Experiments using SCDAP/RELAP5", Paper 10289, Proceedings of ICAPP '10, San Diego, USA, June 13-17, 2010.

[26] J. Birchley and L Fernandez-Moguel, "Simulation of Air Oxidation during a Reactor Accident Sequence: Part 1 – Phenomenology and Model development", Ann. Nucl. Energy, 40, 163-170 (2012).

[27] R. Pawel, J. Cathcart and R. McKee, "The Kinetics of Oxidation of Zircaloy-4 in Steam at High Temperatures", J. of Electrochemical Soc., 126, 1105-1111, (1979).

[28] V. Urbanic and T. Heidrick, "High-Temperature Oxidation of Zircaloy-2 and Zircaloy-4 in Steam, J. Nuclear Materials, 75, 251-261, (1978).

[29] S. Leistikow, G. Schanz, "Oxidation kinetics and related phenomena of zircaloy-4 fuel cladding exposed to high temperature steam and hydrogen-steam mixtures under PWR accident conditions", Nucl. Engrg. Des. 103, 65-84 (1987).

[30] H. Uetsuka, and P. Hofmann, "Reaction Kinetics of Zircaloy-4 in a 25% O2 / 75% Ar Gas Mixture under Isothermal Conditions". Forschungszentrum Karlsruhe Report KfK 3917, (1985).

[31] Steinbrueck, M., Stegmeier, U. and Ziegler, T., 2007. "Prototypical Experiments on Air Oxidation of Zircaloy-4 at High Temperature". Forschungszentrum Karlsruhe Report FZKA 7257.

[32] L. Fernandez-Moguel and J. Birchley, "Simulation of Air Oxidation during a Reactor Accident Sequence: Part 2 – Analysis of PARAMETER-SF4 Air Ingress Experiment using RELAP/SCDAPSIM", Ann. Nucl. Energy, 40, 141-152 (2012).